

See discussions, stats, and author profiles for this publication at: <https://www.researchgate.net/publication/41163916>

# Highly Ordered and Stable Layered “Polymer Nanosheets” Constructed with Amorphous Side Chains and $\pi-\pi$ Stacking of Functional Groups in Ternary Comb Copolymers

ARTICLE *in* THE JOURNAL OF PHYSICAL CHEMISTRY B · FEBRUARY 2010

Impact Factor: 3.3 · DOI: 10.1021/jp9093782 · Source: PubMed

---

CITATIONS

10

READS

48

## 6 AUTHORS, INCLUDING:



Atsuhiro Fujimori

Saitama University

143 PUBLICATIONS 652 CITATIONS

[SEE PROFILE](#)



Hiroko Hoshizawa

Shinshu University

14 PUBLICATIONS 57 CITATIONS

[SEE PROFILE](#)

# 1 Highly Ordered and Stable Layered “Polymer Nanosheets” Constructed with Amorphous 2 Side Chains and $\pi-\pi$ Stacking of Functional Groups in Ternary Comb Copolymers

3 Atsuhiro Fujimori,\* Hiroko Hoshizawa, Satoshi Kobayashi, and Natsuki Sato

4 Graduate School of Science and Engineering, Yamagata University, Jonan 4-3-16, Yonezawa,  
5 Yamagata, 992-8510, Japan

6 Kaname Kanai<sup>‡</sup> and Yukio Ouchi

7 Department of Chemistry, Graduate School of Science, Nagoya University, Furo-cho, Chikusa-ku,  
8 Nagoya 464-8602, Japan

9 Received: September 30, 2009; Revised Manuscript Received: January 12, 2010

10 We have developed a highly stable, layered structure for ternary copolymers in Langmuir–Blodgett (LB)  
11 films at a nanometer scale, with substantial durability over the long-term. In these ternary copolymer LB  
12 films, amorphous side chains support the layered structure, and the distance between the layers is controlled  
13 at the nanometer scale by the composition of hydrogenated and fluorinated side chains. In the present study,  
14 the fine structures of newly synthesized ternary comb copolymers with a carbazole ring in the solid state and  
15 molecular orientations in the LB films were investigated using wide-angle X-ray diffraction (WAXD), small-  
16 angle X-ray scattering (SAXS), surface pressure–area ( $\pi-A$ ) isotherms, in-plane and out-of-plane X-ray  
17 diffraction (XRD), and atomic force microscopy (AFM). The WAXD results identified two short-spacing  
18 peaks related to the formation of the subcells for both the fluorinated and hydrogenated side chains. Further,  
19 SAXS measurements indicated that these ternary copolymers formed a highly ordered layer structure. In  
20 addition, monolayers on the water surface of these ternary copolymers were highly condensed. From the  
21 results of in-plane XRD and AFM, it was determined that the side chains and side-chain crystals could not  
22 form phase-separated structures in two-dimensional films. These structural features may result from  
23 enhancement of  $\pi-\pi$  interactions between the arranged carbazole rings. The side chains of the copolymers  
24 in the two-dimensional films are apparently in a miscible state, and monolayers form a homogeneous amorphous  
25 surface because of cancellation of differences in van der Waals forces between the two types of side chains.  
26 As a result, formation of a highly ordered layer structure in copolymer films having substantial durability  
27 over the long term is realized because amorphous side chains support the layer structure in the LB multilayers.  
28 Further, control of long spacing at a subnanometer level becomes possible due to changes in the tilt angle of  
29 the side chains, depending on their fluorocarbon content.

## 30 Introduction

31 Comb polymers are attractive materials because of differences  
32 in their solid-state nature between the main chains and the side  
33 chains, generally resulting in long-range phase-segregated  
34 structures.<sup>1</sup> Crystalline main-chain polymers with amorphous  
35 side chains<sup>2</sup> and amorphous main-chain polymers with crystal-  
36 line side chains<sup>3</sup> have been extensively studied and well  
37 reviewed in terms of chemistry<sup>4</sup> and physical properties.<sup>5</sup>  
38 Movement of the crystalline segments is more or less inhibited  
39 by the amorphous section; thus, the various segregated structures  
40 are formed from similar materials. Much attention has been paid  
41 to the “crystalline–crystalline” comb polymers,<sup>6</sup> especially the  
42 aromatic main-chain polymers,<sup>7</sup> because the packing structure  
43 of the bulky aromatic polymer main chain can be varied by  
44 varying the crystallinity of the side chains.

45 Characteristics of the structure of side-chain crystalline comb  
46 polymers include a layered structure along the *c*-axis and side-  
47 chain subcells in the *ab*-plane.<sup>8</sup> This subcell structure<sup>9</sup> of the  
48 side chains has the form of a two-dimensional lattice, and the  
49 layer structure along the *c*-axis often reflects the long spacing

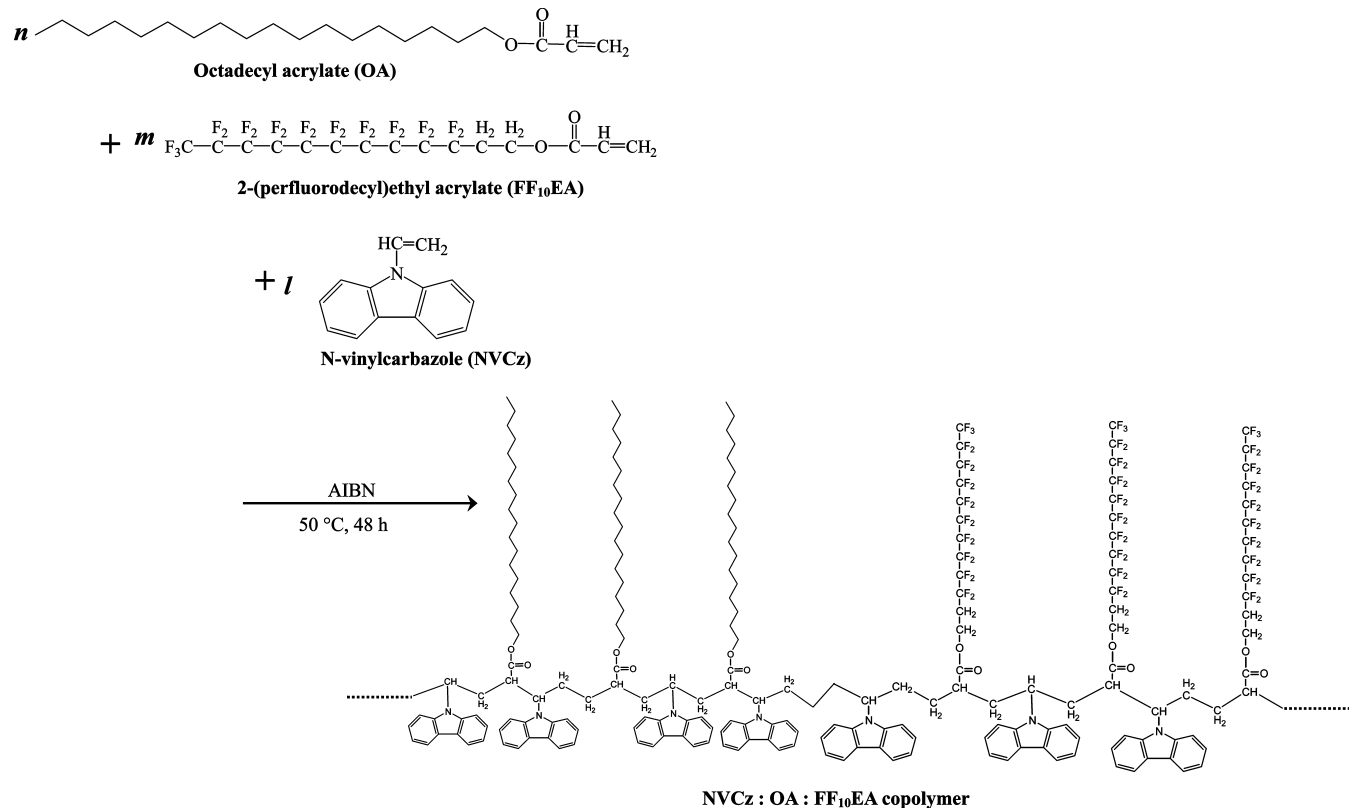
50 between the main chains in the accumulated double-layer  
51 structure. These structural features reflect aspects of both three-  
52 dimensional crystals and two-dimensional molecular films and  
53 also of long-chain compounds with low molecular weight and  
54 the resultant comb polymers polymerized from these long-chain  
55 monomers. These structural formations arise from van der Waals  
56 interactions between the long side chains. Poly(octadecyl)-based  
57 materials prepared through cocrystallization with another hy-  
58 drocarbon in the same crystalline lattice have found numerous  
59 industrial applications, including pour-point depressants for  
60 lubricating oils or fuels, rheological modifiers, and additives in  
61 petroleum products.<sup>10</sup>

62 In recent years, researchers have begun investigating the use  
63 of poly-*N*-vinylcarbazole (PNVCz) for organic light-emitting  
64 diodes and organic transistors and as host compounds for organic  
65 electroluminescence,<sup>11</sup> because it is well-known that PNVCz  
66 exhibits properties identical to those of organic semiconductors.<sup>12</sup>  
67 Further, it is expected that PNVCz could be used as a hologram  
68 memory material because of the high refractive index (greater  
69 than 1.68) of its monomer.<sup>13</sup>

70 It is essential to control the molecular orientation and  
71 arrangement at the monomolecular level to efficiently derive  
72 the functionality of these organic molecular devices. However,  
73 it can be difficult to control the molecular arrangement and

\* To whom correspondence should be addressed. Tel. and Fax: +81-238-26-3073. E-mail: fujimori@yz.yzmzgata-u.ac.jp.

<sup>‡</sup> Present address: Research Core for Interdisciplinary Science, Okayama University.

**SCHEME 1: Polymerization Reaction of NVCz:OA:FF<sub>10</sub>EA Copolymers**

homopolymer packing because PNVCz easily forms an amorphous polymer.<sup>14</sup>

Previously, we have investigated the control of the formation of solid-state structures and organized films for newly synthesized comb copolymers containing hydrogenated and fluorinated side chains.<sup>15</sup> These comb polymers form a side-chain crystal in the bulk state through van der Waals interactions between the side chains and the highly stable condensed monolayer at the air/water interface. In addition, we have incorporated both bulky and flat functional groups into the main chains of side-chain crystalline polymers and succeeded in controlling the arrangement of bulky groups at the molecular level, despite the low crystallinity of the polymers.<sup>16</sup>

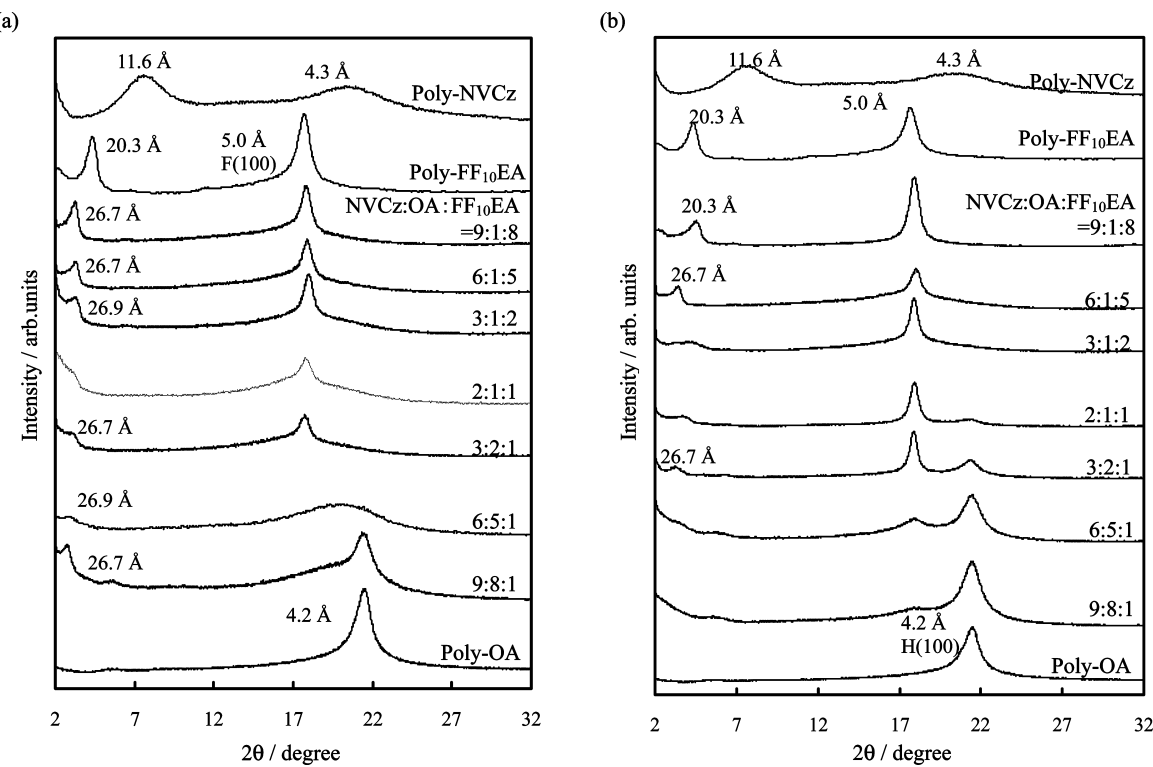
In this study, the fine structures of the synthesized ternary comb polymers containing *N*-vinylcarbazole (NVCz) in the main chains, obtained through copolymerization using hydrogenated and fluorinated long-chain vinyl compounds, were investigated in the solid state using wide-angle X-ray diffraction (WAXD) and small-angle X-ray scattering (SAXS). Further, the molecular arrangements and morphologies of the organized molecular films in ternary comb copolymers containing NVCz units were estimated using surface pressure-area ( $\pi$ - $A$ ) isotherms, in-plane and out-of-plane X-ray diffraction (XRD), polarized near-edge X-ray absorption fine structure (NEXAFS) spectroscopy, and atomic force microscopy (AFM). Generally, hydrogenated and fluorinated side chains coexist as an immiscible system.<sup>17</sup> Initially, we attempted to develop a layered polymer organization, while controlling both the arrangement of the bulky groups and the phase-separated patterning surface. However, formation of a highly ordered layer structure in the copolymer films having substantial durability over the long term resulted, with an amorphous surface constructed by apparently miscible side chains supporting the layer structure in the Langmuir–Blodgett (LB) multilayers. This was newly termed a “polymer nanosheet”

material.<sup>18</sup> In addition, control of the long period along the *c*-axis at the subnanometer level was made possible by varying the tilt angle of the side chains based on their fluorocarbon content. Further, we discuss the possibilities for utilization of these layered organizations of ternary copolymers as new polymer nanomaterials.

**Experimental Section**

**Materials.** The ternary comb copolymers used in this study were obtained through copolymerization of NVCz with octadecyl acrylate (OA) and 2-(perfluorodecyl)ethyl acrylate (FF<sub>10</sub>EA) at various monomer ratios. Copolymerization was carried out in an acetone solution at 50 °C for 48 h using azobisisobutyronitrile (AIBN) as an initiator (Scheme 1). The monomers and the initiator were purchased from Tokyo Kasei Co. Ltd. and Daikin Fine Chemicals Co. Ltd. and were used without further purification. The precipitated polymers were washed with acetone until they were free of monomers. The syndiotactic poly-FF<sub>10</sub>EA homopolymer was obtained through 1.0 M rad <sup>60</sup>Co  $\gamma$ -ray irradiated postpolymerization, as described previously.<sup>19</sup>  $\gamma$ -ray irradiation was carried out at the Japan Atomic Energy Institute at Takasaki. Ternary comb copolymer compositions were determined using <sup>1</sup>H NMR (Nihon Denshi Co. Ltd. EX270 NMR) spectroscopy. The tacticity of the fluorinated homopolymer obtained by <sup>1</sup>H NMR analysis was found to be almost syndiotactic (diad: 57.4%), based on the reference. In this study, we synthesized ternary copolymers with two series of molecular weights estimated at approximately  $M_w = 4.43 \times 10^4$  and  $4.93 \times 10^3$  ( $M_w/M_n \approx 2.14$  and 1.17, respectively), based on GPC (JASCO-860-CO) measurements. The molecular weights of the fluorinated homopolymers of the FF<sub>10</sub>EA units were estimated to be >1000. These values were estimated from the intrinsic viscosity  $[\eta]$ , which is equal to 0.12–0.54 for these trifluoroacetic acid solutions at 30 °C, using

## Ordered and Stable Layered “Polymer Nanosheets”

*J. Phys. Chem. B*, Vol. xxx, No. xx, XXXX C**Figure 1.** Powder XRD profiles of NVCz:OA:FF<sub>10</sub>EA copolymers at low (a) and high (b) molecular weight.

141 the relation  $[\eta] = KM^\alpha$ , where  $K = 0.24\text{--}0.25 \times 10^{-4}$  and  $\alpha$   
 142 = 0.75–0.78. The values of  $K$  and  $\alpha$  were assumed based on  
 143 the viscosity-averaged molecular weight of polyalkyl acrylate.<sup>20</sup>

144 According to the theoretical  $Q$ – $e$  scheme proposed by Alfrey  
 145 and Price,<sup>21</sup> these ternary comb polymers form alternating  
 146 copolymers of NVCz and long-chain acrylates. In this case, the  
 147  $e$  values of NVCz, OA, and FF<sub>10</sub>EA were –1.40, +1.12, and  
 148 +0.66, respectively. Thus, it appears that the NVCz:long-chain  
 149 acrylate copolymers formed nearly ideal alternating copolymers,  
 150 particularly in a 2:1:1 monomer ratio. However, hydrogenated  
 151 and fluorinated side-chain units of the single-polymer chains  
 152 randomly occurred in the main chains because of the equal  
 153 reaction affinities of both long-chain acrylates for radical  
 154 polymerization.

155 **Structural Estimation of Bulk Copolymers.** The packing  
 156 modes of several copolymers in the crystalline phase were  
 157 examined using wide-angle X-ray powder diffraction measure-  
 158 ments with a Rigaku Rad-rA diffractometer, equipped with a  
 159 graphite monochromator, with Cu K $\alpha$  radiation at 40 kV and  
 160 100 mA. The layer structures of the comb copolymers were  
 161 characterized using SAXS (M18XHF; MAC Science Co.),  
 162 consisting of an 18 kW rotating-anode X-ray generator with a  
 163 Cu target (wavelength,  $\lambda = 0.154$  nm) operated at 50 kV and  
 164 300 mA. This instrument comprised a pyrographite monochro-  
 165 mator, pinhole collimation system ( $\phi \sim 0.3, 0.3, 1.1$  mm),  
 166 vacuum chamber for the scattered beam path and a two-  
 167 dimensional imaging plate detector (DIP-220). The sample-to-  
 168 detector distance was adjusted to 710 mm. The exposure time  
 169 for each sample was 30 min. For the SAXS measurements, a  
 170 sample of approximately 1.0 mm thickness was placed in the  
 171 sample holder so that its position remained unchanged.<sup>22</sup>

172 **Formation of Copolymer Monolayers on the Water**  
**173 Surface and Molecular Arrangement in the Films.** Mono-

177 polymers were measured with a film balance (Kyowa Kaimen  
 178 Kagaku Co. Ltd., compression speed: 3 cm/min) at 15 °C. The  
 179 fluorinated comb copolymers formed extremely condensed  
 180 monolayers. These monolayers were transferred to solid sub-  
 181 strates at 15 °C and a surface pressure of 15–25 mN·m<sup>–1</sup> by  
 182 the Langmuir–Blodgett (LB)<sup>23,24</sup> and surface-lowering meth-  
 183 ods<sup>25</sup> to obtain the alternating Y-type film and the nonalternating  
 184 Z-type films, respectively. The hydrophobic side chains on the  
 185 outermost surface of the Z-type films were exposed to the air.

186 The surface morphologies of the transferred films were  
 187 observed using a scanning probe microscope (Seiko Instruments  
 188 SPA300 with an SPI-3800 probe station), using microfabricated  
 189 rectangular Si cantilevers with integrated pyramidal tips at a  
 190 constant force of 1.4 N·m<sup>–1</sup>. The long spacings of the layered  
 191 structures of the films on the glass substrates were measured  
 192 using an out-of-plane X-ray diffractometer (Rigaku Rad-rA, Cu  
 193 K $\alpha$  radiation, 40 kV, 100 mA) equipped with a graphite  
 194 monochromator. The in-plane spacings of the two-dimensional  
 195 lattices of the films were determined using an X-ray diffracto-  
 196 meter at various geometrical arrangements<sup>26</sup> (Bruker AXS,  
 197 MXP-BX, Cu K $\alpha$  radiation, 40 kV, 40 mA, an instrument  
 198 specially made to order) equipped with a parabolic graded  
 199 multilayer mirror. NEXAFS spectra<sup>27,28</sup> of the LB films were  
 200 obtained along the BL-7A soft X-ray beamline with synchrotron  
 201 radiation from a bending-magnet source at the parallel-polarized,  
 202 grazing incidence monochromator station of the Photon Factory  
 203 at the High-Energy Accelerator Research Organization (KEK-  
 204 PF) National Laboratory. The C NEXAFS spectra were  
 205 measured by varying the incident angle in the photon energy  
 206 region of 275–325, in the total electron yield (TEY) mode under  
 207 a vacuum in the 10<sup>–8</sup> torr range.

**Results and Discussion**

208 **Fine Structures of the Ternary Comb Copolymers in the**  
**209 Bulk State.** Figure 1 shows the WAXD profiles of the ternary

210 F1

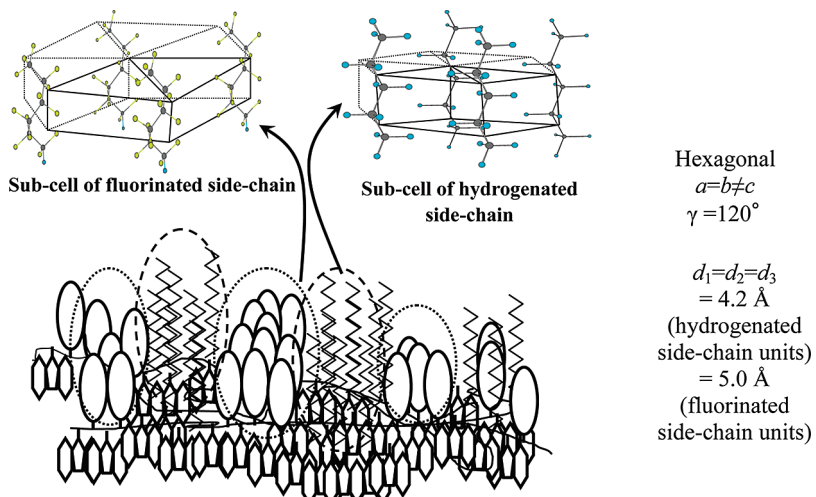


**Figure 2.** Schematic illustration of subcell structure and aggregated structure in the solid state of NVCz:OA:FF<sub>10</sub>EA copolymers.

211 comb copolymers with low and high molecular weights containing NVCz with various side-chain ratios. From these profiles, 212 systematic changes in the short-spacing regions can be discerned 213 with copolymerization ratio. Further, we concluded that PNVCz 214 forms an amorphous polymer, judging from the appearance of 215 two halos around 4.3 and 11.6 Å and the absence of any 216 crystalline peaks.

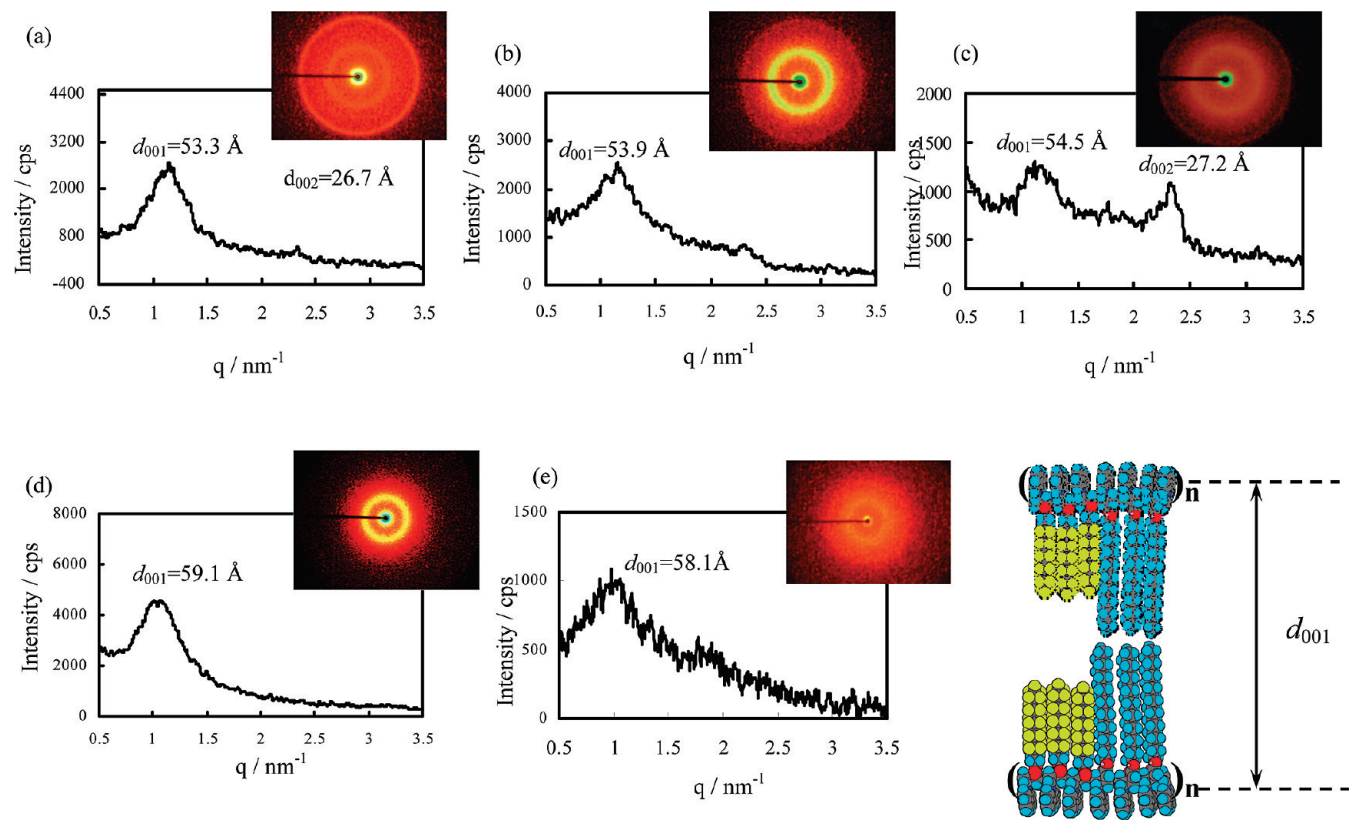
217 In addition, the profiles of poly-OA and poly-FF<sub>10</sub>EA contained short-spacing peaks at 4.2 and 5.0 Å, related to the 218 subcell formations of the two side chains. According to Platé's 219 review, these peaks generally correspond to (100) reflections 220 of the two-dimensional hexagonal lattice.<sup>29</sup> In profiles of 221 copolymers with high molecular weights, both short-spacing 222 peaks at 4.2 and 5.0 Å were generally confirmed, especially 223 for those with NVCz:OA:FF<sub>10</sub>EA ratios of 2:1:1, 3:2:1, 6:5:1, 224 and 9:8:1. However, low-molecular-weight copolymers with the 225 same components nearly always produced a single short-spacing 226 peak with a halo of a few degrees to either side, indicating higher 227 crystallinity of the copolymers with high molecular weights. In 228 the small-angle region, long-spacing peaks were clearly observed 229 in the profile of poly-FF<sub>10</sub>EA at approximately 20.3 Å, whereas 230 no peaks were observed on the low-angle area of the profile of 231 poly-OA. Poly-FF<sub>10</sub>EA forms a highly ordered layer structure 232 along the direction of the *c*-axis. Consistent with previous 233 results, it appears that these long-spacing peaks are related to 234 the (002) reflection<sup>30</sup> because poly-FF<sub>10</sub>EA forms a double- 235 layer structure and the calculated length of the fluorocarbon side 236 chain is approximately 20 Å. On the basis of computer 237 simulations, the *d* spacing associated with the (001) reflection 238 of poly-OA was expected to be approximately 50 Å 239 (double-layer spacing), although poly-OA did not form a layered 240 structure in the bulk state. For copolymers, long spacing based 241 on the formation of a layered structure occurs until a copoly- 242 merization ratio of approximately 20.3–26.9 Å is reached. 243 Further discussion of the long period along the *c*-axis is 244 supported by the SAXS measurements presented below.

245 On the basis of the WAXD measurements, models for the 246 molecular arrangement and side-chain packing of the ternary 247 comb copolymers are shown in Figure 2. The side chains of 248 both the hydro- and fluorocarbons of all of the copolymers 249 synthesized in this study are packed two-dimensionally in 250 hexagonal subcells at a lattice spacing of 4.2 and 5.0 Å, 251 respectively. This result highlights the dominant influence of 252 the van der Waals interactions between the two side chains on 253 the bulk crystal structure formation.

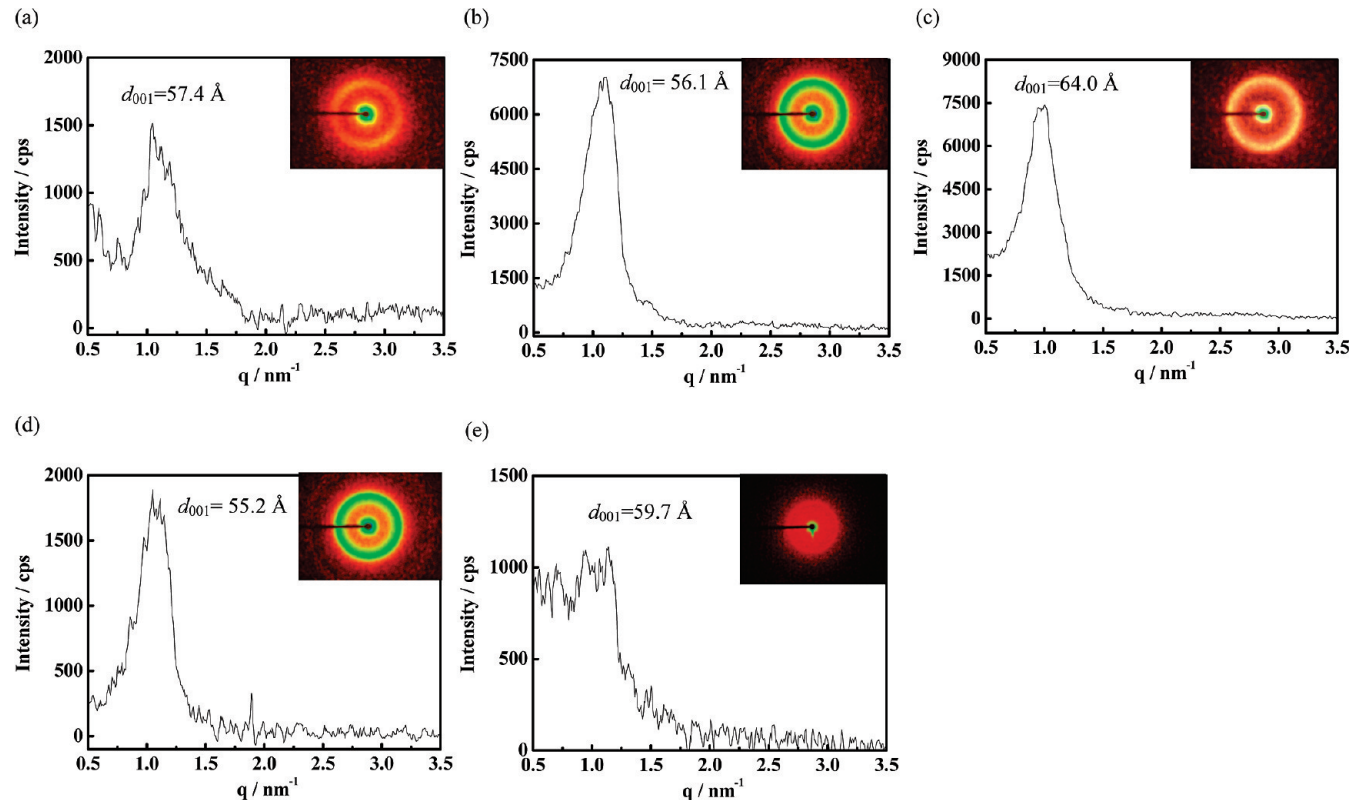
The results of the SAXS measurements (Figures 3 and 4) indicated that the NVCz:OA:FF<sub>10</sub>EA copolymers with both low and high molecular weights form double-layer structures because a bilayer spacing peak appears at >50 Å in each profile. A simple model of a double-layer structure for the NVCz:OA:FF<sub>10</sub>EA copolymer is shown in Figure 3. Comparing the ternary copolymers with low and high molecular weights, low intensity signals are confirmed in the SAXS profiles of ternary comb copolymers with low molecular weights, indicating small differences in the crystal/amorphous electron densities of these crystals (Figure 3). For the present system, it is hypothesized that the crystal and amorphous regions nearly correspond to the side-chain and main-chain regions, respectively. On the basis of the WAXD results, formation of the side-chain crystal is clearly confirmed, and the ternary copolymers with high molecular weights indicate relatively high side-chain crystallinity. Polyacrylic acid is typical of the amorphous polymers; i.e., differences in the peak intensities in the SAXS profiles of these ternary copolymers indicate electron density between the side-chain and main-chain regions, and the high crystallinity of side-chain units in the copolymers with high molecular weights suggested by WAXD is supported (Figure 4).

Figure 5 presents a plot of hydrogenated side-chain content vs long spacing, estimated using SAXS profiles of NVCz:OA:FF<sub>10</sub>EA copolymers and a schematic illustration of the double-layer structure of the ternary comb copolymers. This result indicates a tilted orientation of the side chain, especially the longer hydrogenated chains. On the basis of a simple simulation of the molecular length, the tilt angle of the hydrogenated side chain slightly varies over 28–30°, depending on the side-chain content.

**Molecular Arrangement and Surface Morphology of Organized Molecular Films of Ternary Comb Copolymers.** On the basis of the above experimental findings, we attempted to utilize ternary comb copolymers containing NVCz units as materials for the formation of monolayers on the water surface. Figure 6 shows the  $\pi$ -*A* isotherms for monolayers of the NVCz:OA:FF<sub>10</sub>EA ternary copolymers with low and high molecular weights on distilled water at 15 °C. It has been observed that these ternary comb polymer monolayers become highly stabilized and form condensed films on the water surface. For both high- and low-molecular-weight polymers, the monolayers of the ternary copolymers with a high OA content exhibited a relatively low collapsed surface pressure, particularly the NVCz:



**Figure 3.** Small-angle X-ray scattering profiles and patterns of NVCz:OA:FF<sub>10</sub>EA copolymers = (a) 6:1:5, (b) 3:1:2, (c) 2:1:1, (d) 3:2:1, and (e) 6:5:1 at low molecular weight and schematic illustration of the double-layer structure for copolymers.

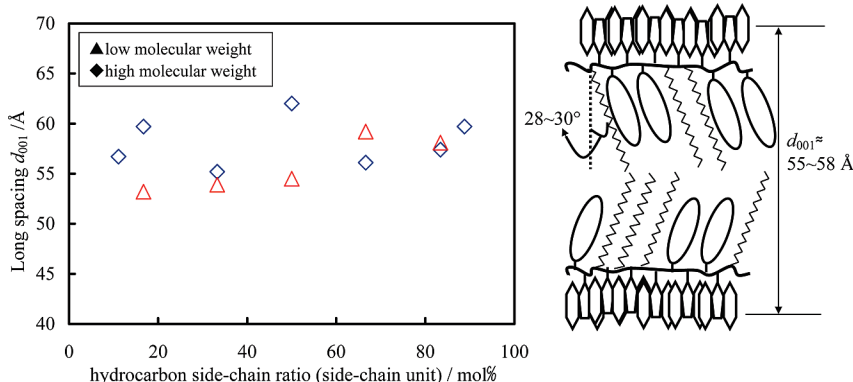


**Figure 4.** Small-angle X-ray scattering profiles and patterns of NVCz:OA:FF<sub>10</sub>EA copolymers = (a) 6:1:5, (b) 3:1:2, (c) 2:1:1, (d) 3:2:1, and (e) 6:5:1 at high molecular weight.

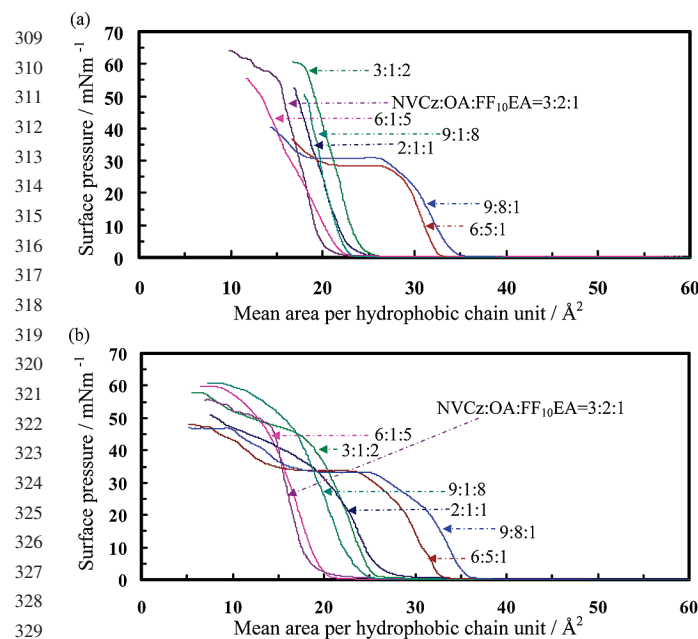
301 OA:FF<sub>10</sub>EA = 6:5:1 and 9:8:1 copolymers. In addition, because  
 302 the distributions of the limiting areas of the hydrophobic side  
 303 chains of the copolymers with low molecular weights were  
 304 relatively sharp, ternary copolymers with low molecular weights

generally conform to previous research on two-dimensional molecular film formation on solids.

305 Interestingly, based on the AFM images presented in Figures  
 306 7 and 8, the Z-type monolayers of NVCz:OA:FF<sub>10</sub>EA copoly-  
 307  
 308 F7-8



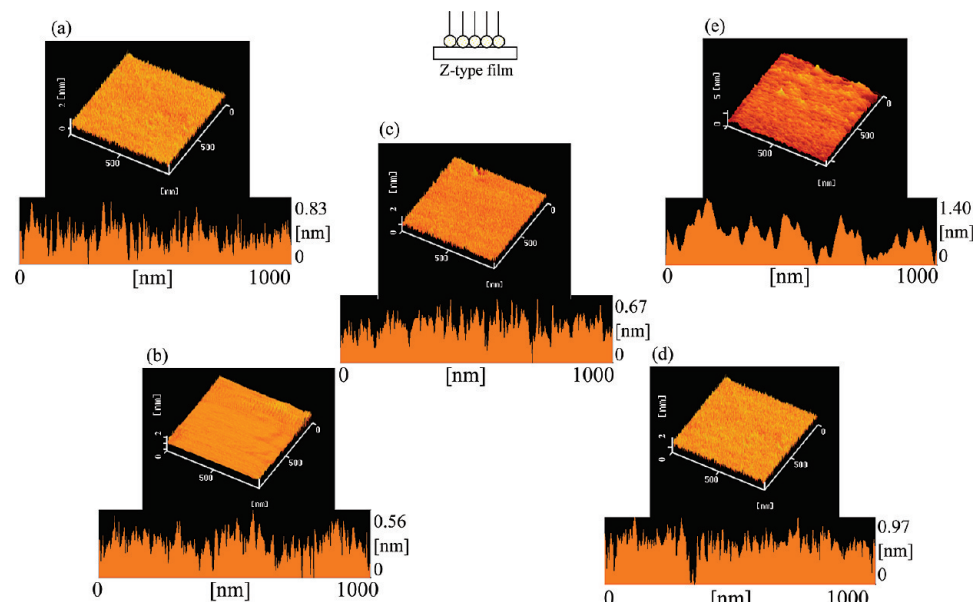
**Figure 5.** Plot of hydrogenated side-chain content vs long spacing estimated by SAXS of NVCz:OA:FF<sub>10</sub>EA copolymers and schematic illustration of the double-layer structure for copolymers.



**Figure 6.** Surface pressure-area isotherms of monolayers on the water surface of NVCz:OA:FF<sub>10</sub>EA copolymers with low (a) and high (b) molecular weight at 15 °C.

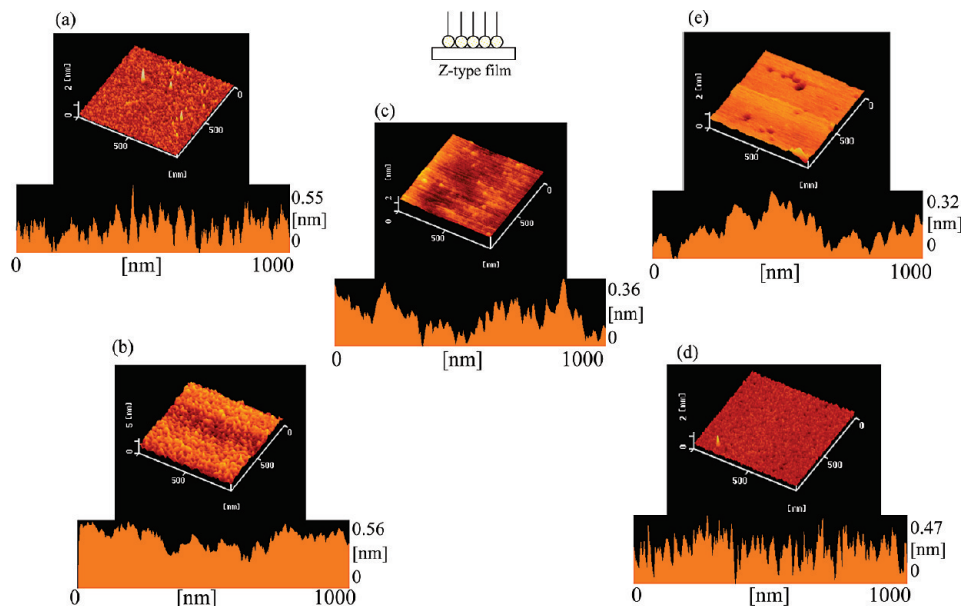
mers with both low and high molecular weights formed remarkably flat and homogeneous surfaces. Figure 7 shows AFM images for several transferred monolayers on a solid of low-molecular-weight ternary comb copolymers containing NVCz. Generally, polymer blends or copolymers having both hydrocarbon and fluorocarbon chains have a phase-separated structure because of the lack of miscibility between these chain types. Previously, we have also observed phase-separated surfaces for monolayers of copolymers obtained by copolymerization of OA and FF<sub>10</sub>EA.<sup>15</sup> However, for this system, quite flat and homogeneous surface morphologies were observed over the mesoscopic probing areas. These apparently miscible surfaces were independent of the copolymerization ratio. These results were almost the same for monolayers of a ternary copolymer with high molecular weight, although subtle increases in surface roughness were confirmed (Figure 8).

Figure 9 presents quite interesting results for in-plane X-ray diffraction of LB multilayers of ternary copolymers with low molecular weight, conducted to estimate side-chain crystallinity in the film. As shown in the inset figure, we have previously reported formation of both hydrogenated and fluorinated side-chain crystals in phase-separated binary copolymer films polymerized by OA and FF<sub>10</sub>EA at the few tens of nanometers scale.<sup>31</sup> In most cases, formation of condensed “island” regions



**Figure 7.** AFM images of several Z-type monolayers on the mica substrate ( $1 \times 1 \mu\text{m}$ ) of NVCz:OA:FF<sub>10</sub>EA = (a) 6:1:5, (b) 3:1:2, (c) 2:1:1, (d) 3:2:1, and (e) 6:5:1 copolymers at low molecular weight.

## Ordered and Stable Layered “Polymer Nanosheets”

*J. Phys. Chem. B*, Vol. xxx, No. xx, XXXX G

**Figure 8.** AFM images of several Z-type monolayers on the mica substrate ( $1 \times 1 \mu\text{m}$ ) of NVCz:OA:FF<sub>10</sub>EA = (a) 6:1:5, (b) 3:1:2, (c) 2:1:1, (d) 3:2:1, and (e) 6:5:1 copolymers at high molecular weight.

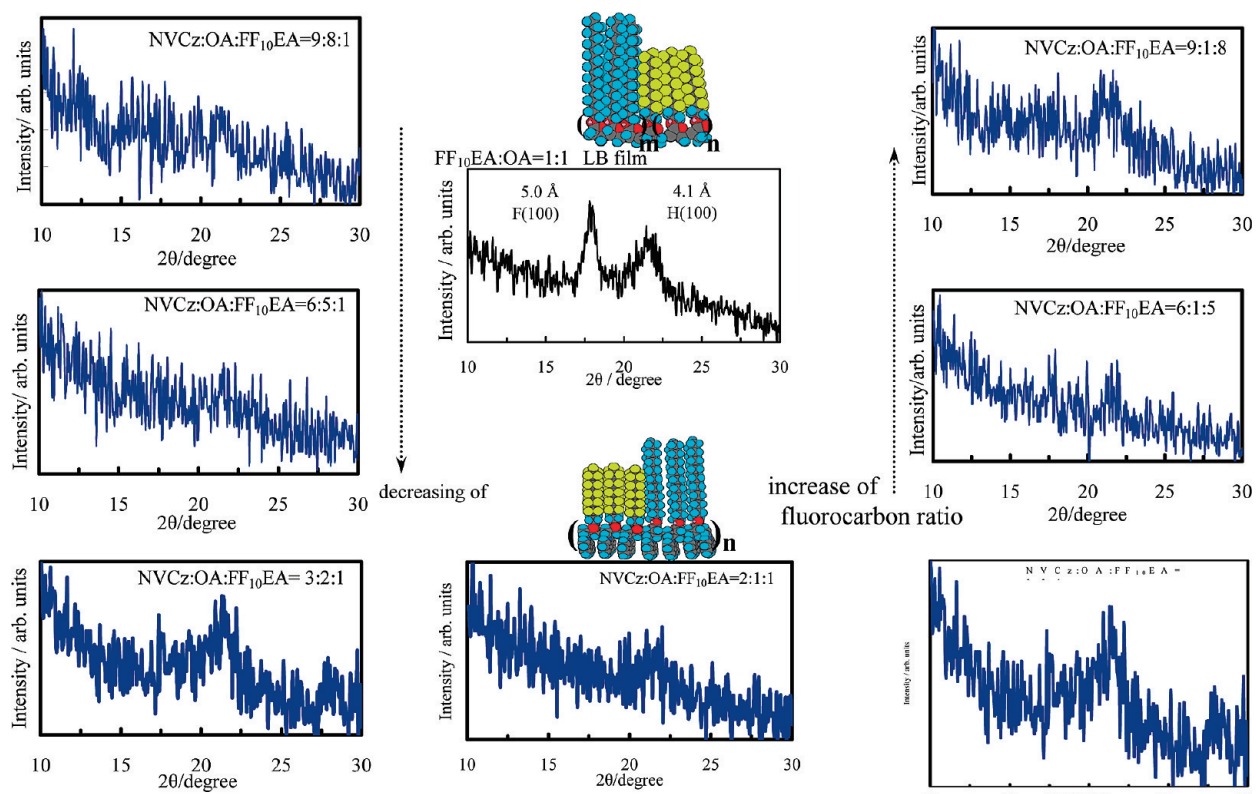


**Figure 9.** In-plane XRD profiles of LB multilayers (20 layers) of NVCz:OA:FF<sub>10</sub>EA ternary comb copolymers. (Inset) In-plane XRD profiles of LB multilayers (20 layers) of OA:FF<sub>10</sub>EA = 1:1 binary comb copolymers.

333 by hydrocarbon chains and surrounding unoriented “sea” regions  
334 by fluorocarbon chains are constructed in the mixed monolayer  
335 surface because there are large differences in van der Waals  
336 interactions between hydrogenated and fluorinated chains.<sup>32</sup> In  
337 the apparent miscible films observed in the present study, it  
338 was found that an amorphous surface was homogeneously  
339 formed, based on the results of in-plane XRD showing only a  
340 halo in the profile.

341 To interpret these phenomena, schematic models are  
342 presented in Figure 10 for NVCz:OA:FF<sub>10</sub>EA ternary comb  
343 copolymers in bulk and in two-dimensional organized films.

In the single polymer chain, hydrogenated and fluorinated  
344 side chains randomly occur in the main chain because these  
345 side chains have equal reaction affinities for radical poly-  
346 merization. In the bulk state, hydrogenated side chains form  
347 a crystal earlier than fluorinated side chains, due to having  
348 stronger van der Waals interactions. Disengaged fluorocarbons  
349 from the “hydrocarbon island” aggregate as a side-chain  
350 crystal later than hydrogenated chains, due to having  
351 relatively weak van der Waals interactions. On the other hand,  
352 carbazole rings arranged as a monolayer on the surface of  
353 the water have relatively strong  $\pi-\pi$  interactions between  
354

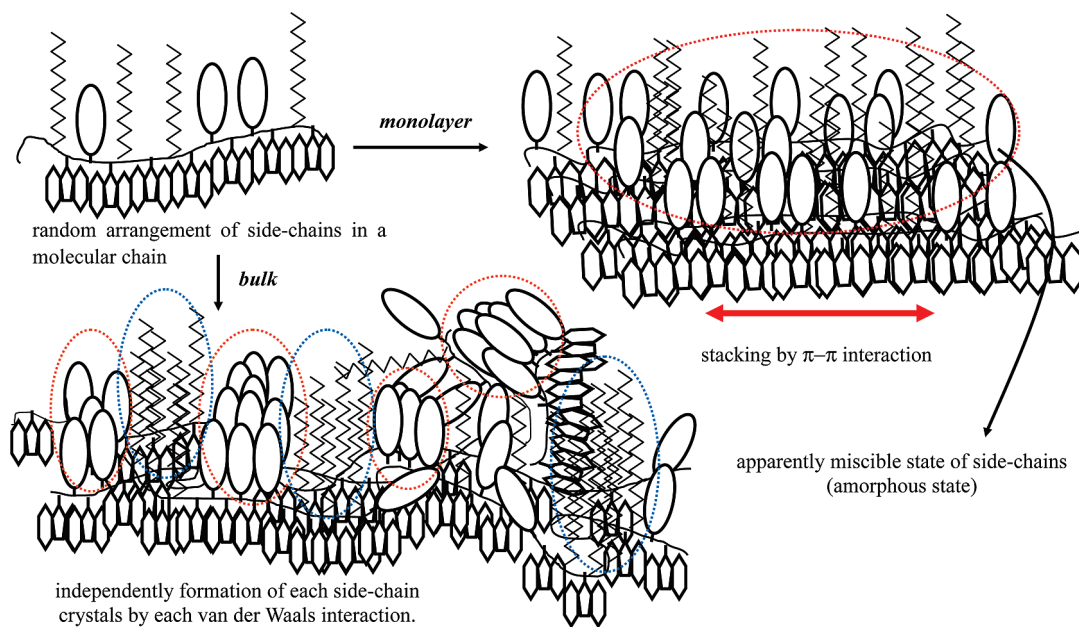


**Figure 10.** Schematic models of structural formation for NVCz:OA:FF<sub>10</sub>EA ternary comb copolymers in bulk and two-dimensional organized film.

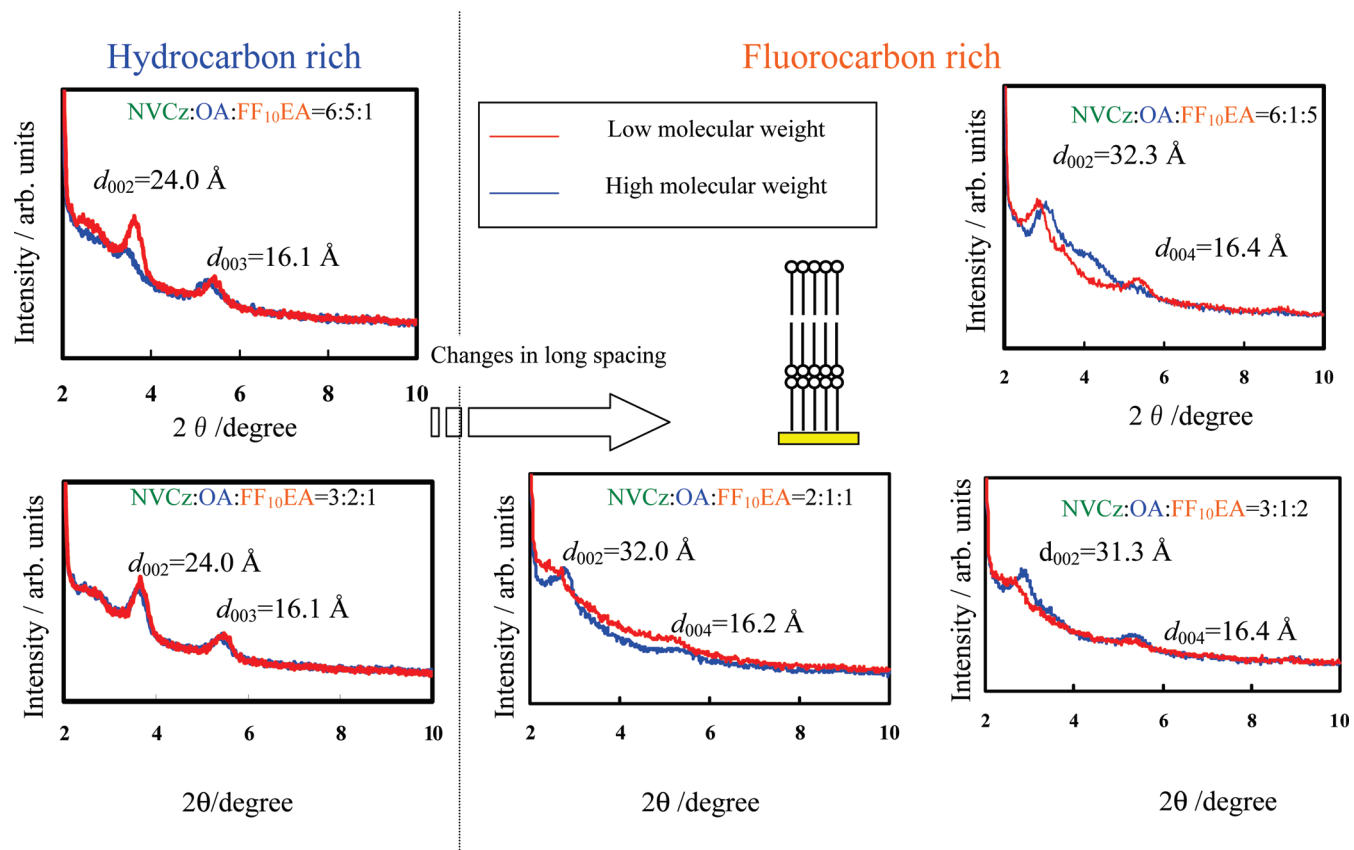


**Figure 11.** Out-of-plane XRD profiles of LB multilayers (20 layers) of NVCz:OA:FF<sub>10</sub>EA ternary comb copolymers.

the ring planes. This  $\pi-\pi$  stacking may bring about a cancellation of differences between the van der Waals interactions for the two types of side chains. We have previously reported changes in side-chain arrangement through  $\pi-\pi$  stacking of functional groups within a  $\pi$ -conjugated system.<sup>16</sup> As a result, a two-dimensional lattice is not able to form because neighboring chains are not always of the same type. The resultant unusual amorphous surface is formed of apparently miscible side chains.

As noted above, it is therefore possible to form a remarkably flat miscible surface constructed from hydrogenated and fluorinated side chains, although the phase-separated patterning surface originally anticipated cannot be formed.

**Construction of Novel “Polymer Nanosheets” with a Highly Ordered Layer Structure with Amorphous Side Chains and  $\pi-\pi$  Stacking of Functional Groups in Ternary Comb Copolymers.** Above, we describe development of an organized polymer monolayer with a flat amorphous surface.

364  
365  
366  
367  
368  
369  
370  
371  
372

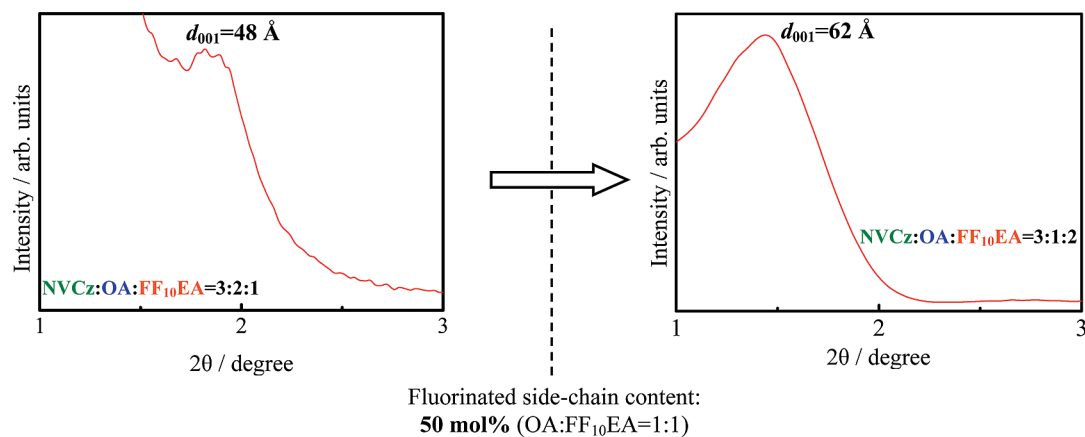


**Figure 12.** Change of first-order diffraction in out-of-plane XRD profiles of LB multilayers at the low-angle side of ternary comb copolymers for NVCz:OA:FF<sub>10</sub>EA = 3:2:1 and 3:1:2 with low molecular weight.

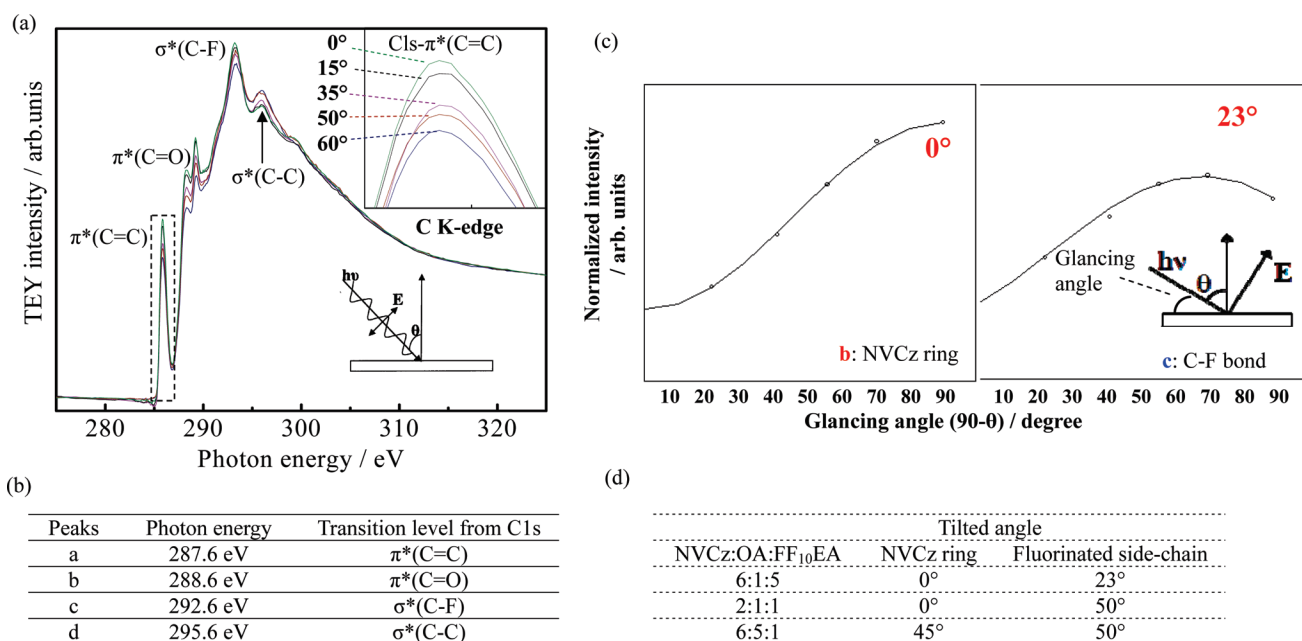


**Figure 13.** (a) C K-edge polarized NEXAFS spectra for the LB film of NVCz:OA:FF<sub>10</sub>EA = 6:5:1 copolymer. (b) Table of deconvoluted transition peaks from C1s. (c) Estimation of orientation angle for (left) the carbazole group and (right) fluorinated side chains in the monolayer of NVCz:OA:FF<sub>10</sub>EA = 6:5:1 copolymer. (d) Table of tilted angles of the carbazole group and fluorinated side chains in the copolymer LB films.

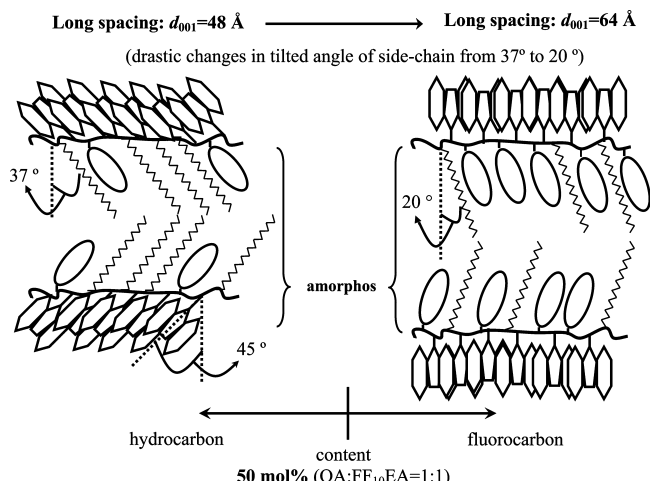
Amorphous polymer LB films can be used to form a stable layered organization at a nanometer scale having substantial durability over the long term. Therefore, we next attempted the formation of a highly stable layered organization of a homogeneous monolayer of ternary comb copolymers using the LB method. The methods used in this study allowed control of both the molecular arrangement and surface morphology at the subnanometer to micrometer scale.

Figure 11 shows out-of-plane XRD profiles of the LB multilayers of NVCz:OA:FF<sub>10</sub>EA ternary comb copolymers. On the basis of these results, formation of a remarkably ordered layered structure along the *c*-axis of the ternary copolymers in the LB film is apparent. LB films of ternary copolymers with both low and high molecular weights clearly exhibited long-spacing peaks associated with  $d_{002}$  and  $d_{003}$ . Interestingly, the  $d_{002}$  reflection peaks shifted to a lower-angle region for a certain content of fluorinated side-chain units. At this point, the  $d_{001}$  values representing bilayer spacing greatly shifted from 48 to 64 Å.

Figure 12 shows change of first-order diffraction peaks in out-of-plane XRD profiles of LB multilayers at the low angle side of ternary comb copolymers for NVCz:OA:FF<sub>10</sub>EA = 3:2:1

and 3:1:2 with low molecular weights. The shift of the first-order diffraction (001) peak is clearly confirmed by this measurement, although an absolute value itself of *d*-spacing value ( $d_{001}$ ) estimated by the Bragg equation at the low-angle region is not always accurate. These results support the above speculation related to changes in layer spacing depending on the copolymerization ratios.

Figure 13 shows the dependence of the C K-edge NEXAFS spectra on the angle of incidence,<sup>27,28,33</sup> using the LB film of the NVCz:OA:FF<sub>10</sub>EA = 6:5:1 copolymer as a typical example, to directly examine the orientation of the carbazole rings. The existence of incident angle dependency in polarized NEXAFS spectra indicates the formation of a highly ordered arrangement of corresponding functional groups or chemical bonds.<sup>16,28,33</sup> In the present case, formation of oriented carbazole rings through  $\pi-\pi$  stacking can be demonstrated. Essentially, NEXAFS spectroscopy does not estimate intermolecular interaction. However, the proof itself of ordering of the  $\pi$ -conjugated bulky and flat ring originates in the occurrence of interaction between rings. Especially, in this case, the three-dimensional crystal of ternary copolymers can not arrange carbazole rings in order.



**Figure 14.** Schematic illustrations of layer structure for NVCz:OA:FF<sub>10</sub>EA ternary comb copolymers in LB film.

The functionalized groups form the highly ordered orientation by method of organized molecular films, and this finding is proven by polarized NEXAFS. In addition, proof of arrangement formation of these  $\pi$ -conjugated rings estimated by polarized NEXAFS spectroscopy means ordering of the  $\pi$ -orbital. That is to say, polarized NEXAFS results indirectly connect recognition of formation of the  $\pi$ - $\pi$  stacking structure between functionalized groups. The NEXAFS spectra of the C1s to  $\pi^*(\text{C}=\text{C})$  transition strongly depend on the incident angle. Because the C=C bond exists only in the carbazole rings, the dependence of this transition reflects a regular arrangement of the carbazole rings (Figure 13a). The peak at 285.5 eV (Figure 13b) reaches a maximum at grazing incidence and is weakened at normal incidence. This clear dependence of the C1s to  $\pi^*$  transition indicates a highly ordered orientation of the carbazole groups with a nearly perpendicular orientation of the  $\pi^*$  orbital. The inset in the upper right of Figure 13c shows a plot of the normalized peak intensity vs the incident angle. Regular arrangement of the functional group is evident. Assuming uniaxial orientation, the orientation angle of the carbazole group

was determined by fitting the dependence of the normalized intensity. Assuming a tilt angle of 14.3° of the  $-\text{CF}_2$  plane with respect to the perpendicular direction of the molecular axis of the fluorocarbon (resulting in a 13/6 helical conformation), the orientation angle of the fluorinated side chains was determined. The carbazole group and the fluorinated side chains in this copolymer LB film should be tilted by about by 0–45° and 23–50° with respect to surface normal, respectively (Figure 13d).

Figure 14 shows schematic illustrations of changes in the layer structure of NVCz:OA:FF<sub>10</sub>EA ternary comb copolymers in LB film depending on the side-chain content. On the basis of the results of AFM and in-plane XRD, it was determined that the side chains of these ternary copolymers are apparently miscible through the influence of  $\pi$ - $\pi$  interactions in the two-dimensional plane. Essentially, it appears that the most stable conformation of the hydrogenated side chain may be a remarkably tilted one. Regarding changes in the layer spacing with copolymerization ratio, changes in the tilt angle of the side chains and functional groups depending on the fluorocarbon content were confirmed by a combination of out-of-plane XRD and polarized NEXAFS spectroscopy. When the side-chain content of hydrogenated and fluorinated parts = 1:1, significant changes in the tilt angle of the side chain from 37° to 20°, together with a 45° tilt of the carbazole ring, occurred due to hindrance of a large inclination of the hydrocarbon chains by fluorinated blocks.

Figure 15 shows schematic models of structural formation for three- and two-dimensional molecular arrangements of ternary comb copolymers containing a carbazole ring, focusing on layer structure and in-plane arrangement of the side chains. In the bulk state, independent formation of the side-chain crystals is attained through van der Waals interactions between the side chains. Further, lack of ordering regularity of the hydrocarbons in copolymers with low molecular weight was confirmed. On the other hand, both types of copolymers formed a highly ordered layer structure, based on SAXS results. For the two-dimensional molecular films, an apparently miscible surface and a highly ordered layer structure were formed. This result reflects enhancement of  $\pi$ - $\pi$  interactions between carbazole rings in the two-dimensional plane in organized molecular films.

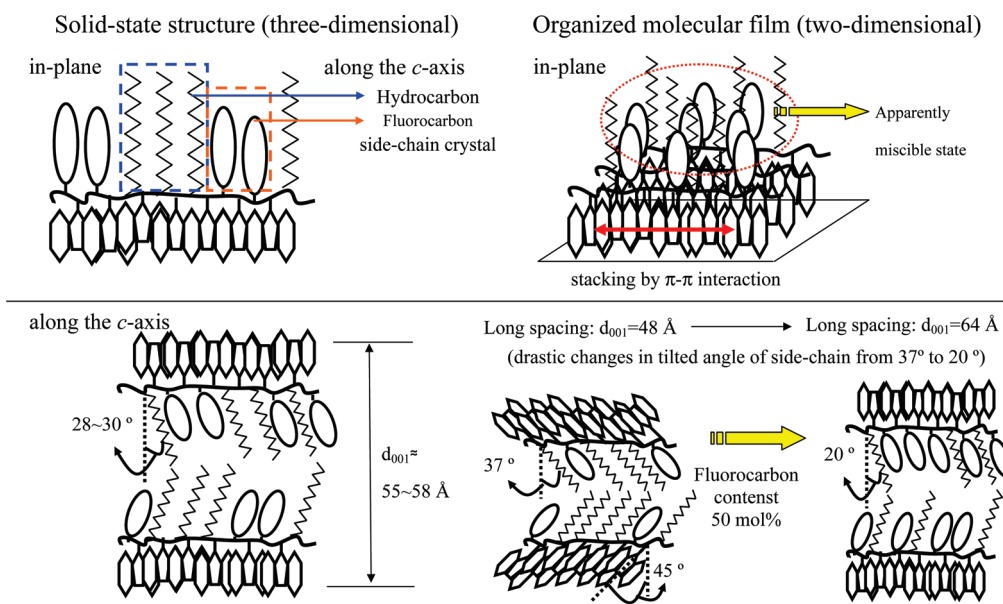


**Figure 15.** Schematic models of structural formation for the ternary comb copolymer containing a carbazole ring in bulk and two-dimensional organized film state.

## Ordered and Stable Layered “Polymer Nanosheets”

As noted above, this method allows development of a highly stable layered organization at a nanometer scale having substantial durability over the long term in LB films of ternary copolymers. On the basis of these experimental findings, it is expected that these copolymers and their organized films can be used as a new functional polymer nanomaterial. We believe that this study is the first in which a novel “polymer nanosheet” material, based on organized molecular films of ternary copolymers with  $\pi$ -conjugated functional groups, particularly with essentially immiscible side chains, has been proposed.

## Conclusions

The fine structures of newly synthesized ternary comb copolymers with a carbazole ring in the solid state and molecular orientation in LB films were investigated using WAXD, SAXS,  $\pi$ -A isotherms, in-plane and out-of-plane XRD, polarized NEXAFS spectroscopy, and AFM observation. A highly stable layered organization at the nanometer scale in LB films of ternary copolymers having substantial durability over the long term has been developed. In these ternary copolymer LB films, amorphous side chains support the layered structure, and the distance between layers can be controlled at a nanometer scale by the composition of hydrogenated and fluorinated side chains.

On the basis of the WAXD results, two short-spacing peaks related to the formation of subcells of both fluorinated and hydrogenated side chains were observed. Further, these ternary copolymers formed a highly ordered layered structure, based on SAXS results. In addition, they formed highly condensed monolayers on the water surface. On the basis of the results of in-plane XRD and AFM, the side chains and side-chain crystals were not able to form phase-separated structures in the two-dimensional films. These structural features may be related to enhancement of  $\pi$ - $\pi$  interactions between the oriented carbazole rings. Therefore, both types of side chains of the copolymers in two-dimensional films are in an apparently miscible state, and the monolayers form a homogeneous amorphous surface due to cancellation of differences in the van der Waals forces between the two types of side chains. As a result, formation of a highly ordered layered structure can be achieved because the amorphous side chains support the layered structure in LB multilayers of copolymer films. Further, control of long spacing at a subnanometer level becomes possible based on changes in the tilt angle of the side chains, depending on the fluorocarbon content.

**Acknowledgment.** The authors thank Prof. K. Amemiya of KEK-PF for help in NEXAFS measurements. This work was performed under approval of the Photon Factory Program Advisory Committee (proposal No. 2008G040).

## References and Notes

- (1) (a) Riess, G.; Hurtrez, G.; Bahadur, P. *Encyclopedia of Polymer Science and Engineering*; Mark, H. F., Kroschwitz, J. I., Eds.; Wiley: New York, 1985; Vol. 2, p 324. (b) Hamley, I. W. *The Physics of Block Copolymers*; Oxford University Press: New York, 1998.
- (2) (a) Watanabe, J.; Sasaki, S.; Uematsu, I. *Polym. J.* **1977**, *9*, 451. (b) Watanabe, J.; Nakata, M.; Watanabe, K.; Uematsu, I. *Polym. J.* **1978**, *10*, 569. (c) Watanabe, J.; Sasaki, S.; Uematsu, I. *Polym. J.* **1977**, *9*, 337. (d) Watanabe, J.; Imai, K.; Gehani, R.; Uematsu, I. *J. Polym. Sci., Part B: Polym. Phys.* **1981**, *19*, 653. (e) Watanabe, J.; Gehani, R.; Uematsu, I. *J. Polym. Sci., Part B: Polym. Phys.* **1981**, *19*, 1817. (f) Gehani, R.; Watanabe, J.; Kasuya, S.; Uematsu, I. *Polym. J.* **1978**, *10*, 871. (g) Sasaki, S.; Nakamura, T.; Miyamoto, M.; Uematsu, I. *Biopolymers* **1973**, *12*, 2657. (h) Sasaki, S.; Nakamura, T.; Uematsu, I. *J. Polym. Sci., Part B: Polym. Phys.* **1979**, *17*, 825. (i) Watanabe, J.; Sasanuma, Y.; Endo, A.; Uematsu, I. *Polymer* **1984**, *25*, 698. (j) Watanabe, J.; Uematsu, I. *Polymer* **1984**, *25*, 698.
- (3) (a) Kaufman, H. S.; Sachen, A. *J. Am. Chem. Soc.* **1948**, *70*, 3147. (b) Overberger, C. G.; Around, L. H.; Wiley, R. H.; Garrett, R. R. *J. Polym. Sci., Part B: Polym. Phys.* **1951**, *7*, 430. (c) Port, W. S.; Hansen, J. E.; Jordan, E. F.; Diety, T. J., Jr.; Swern, D. *J. Polym. Sci., Part B: Polym. Phys.* **1951**, *7*, 207. (d) Overberger, C. G.; Frazier, C.; Mandelman, J.; Smith, H. F. *J. Am. Chem. Soc.* **1953**, *75*, 3326. (e) Inomata, K.; Sakamaki, Y.; Nose, T.; Sasaki, S. *Polym. J.* **1996**, *28*, 986. (f) Inomata, K.; Sakamaki, Y.; Nose, T.; Sasaki, S. *Polym. J.* **1996**, *28*, 992.
- (4) (a) Gao, H.; Matyjaszewski, K. *Prog. Polym. Sci.* **2009**, *34*, 317. (b) Hadjichristidis, N.; Iatrou, H.; Pitsikalis, M.; Mays, J. *Prog. Polym. Sci.* **2006**, *31*, 1068.
- (5) Peleshanko, S.; Tsukruk, V. V. *Prog. Polym. Sci.* **2008**, *33*, 523.
- (6) (a) Watanabe, J.; Ono, H.; Uematsu, I.; Abe, A. *Macromolecules* **1985**, *18*, 2141. (b) Inomata, K.; Sasaki, Y.; Nose, T. *J. Polym. Sci., Part B: Polym. Phys.* **2002**, *40*, 1904. (c) Watanabe, J.; Takashima, Y. *Macromolecules* **1991**, *24*, 3243. (d) Harkness, B. R.; Watanabe, J. *Macromolecules* **1991**, *24*, 6759.
- (7) (a) Ballauff, M. *Angew. Chem., Int. Ed. Engl.* **1987**, *28*, 253. (b) Ebert, M.; Herrmann-Schenk, O.; Wendorff, J.; Ringsdorf, H.; Tscherner, P. *Liq. Cryst.* **1990**, *11*, 249. (c) Watanabe, J.; Harkness, B. R.; Sone, M.; Kricheldorf, H. R. *Macromolecules* **1994**, *27*, 507. (d) Watanabe, J.; Sekine, M.; Nematsu, T.; Sone, M.; Kricheldorf, H. R. *Macromolecules* **1996**, *29*, 4816.
- (8) Neugebauer, D.; Theis, M.; Pakula, T.; Wegner, G.; Matyjaszewski, K. *Macromolecules* **2006**, *39*, 584.
- (9) Vand, V. *Acta Crystallogr.* **1951**, *4*, 465.
- (10) Baskar, G.; Ramya, S.; Mandal, A. *Colloid Polym. Sci.* **2002**, *280*, 886.
- (11) Pearson, J. M.; Stolka, M. *Poly(N-vinylcarbazole)*. *Polymer monograph*; Gordon and Breach: New York, 1981; Vol. 6.
- (12) Choudhury, K. R.; Samoc, M.; Patra, A.; Prasad, P. N. *J. Phys. Chem. B* **2004**, *108*, 1556.
- (13) Laguna, M. T. R.; Gallego, J.; Mendicuti, F.; Saiz, E.; Tarazona, M. P. *Macromolecules* **2006**, *35*, 7782.
- (14) Maertens, C.; Dubois, P.; Jerome, R.; Blanche, P. A.; Lemaire, P. C. *J. Polym. Sci., Part B: Polym. Phys.* **2000**, *38*, 205.
- (15) Masuya, R.; Ninomiya, N.; Fujimori, A.; Nakahara, H.; Masuko, T. *J. Polym. Sci., Part B: Polym. Phys.* **2006**, *44*, 416.
- (16) (a) Fujimori, A.; Sato, N.; Kanai, K.; Ouchi, Y.; Seki, K. *Langmuir* **2009**, *25*, 1112. (b) Hoshizawa, H.; Masuya, R.; Masuko, T.; Fujimori, A. *Polym. Adv. Technol.* **2007**, *18*, 353. (c) Hoshizawa, H.; Fujimori, A. *Colloids Surf. A* **2008**, *322*, 239.
- (17) (a) Fujimori, A.; Nakahara, H. *Chem. Lett.* **2003**, *32*, 2. (b) Fujimori, A.; Kobayashi, S.; Hoshizawa, H.; Masuya, R.; Masuko, T. *Polym. Eng. Sci.* **2007**, *47*, 354.
- (18) (a) Feng, F.; Mitsuishi, M.; Miyashita, T.; Okura, I.; Asai, K.; Amao, Y. *Langmuir* **1999**, *15*, 8673. (b) Budianto, Y.; Aoki, A.; Miyashita, T. *Macromolecules* **2003**, *36*, 8761. (c) Endo, H.; Mitsuishi, M.; Miyashita, T. *J. Mater. Chem.* **2008**, *18*, 1302.
- (19) Fujimori, A.; Saitoh, H.; Shibasaki, Y. *J. Therm. Anal.* **1999**, *57*, 631.
- (20) Fee, J. G.; Port, W. S.; Witnauer, L. P. *J. Polym. Sci.* **1958**, *33*, 95.
- (21) Alfrey, T.; Price, C. C. *J. Polym. Sci.* **1947**, *2*, 101.
- (22) Fujimori, A.; Hayasaka, Y. *Macromolecules* **2008**, *41*, 7606.
- (23) Gaines, G. L., Jr. *Insoluble Monolayers at Liquid Gas Interfaces*; Wiley: New York, 1966.
- (24) Fukuda, K.; Nakahara, H.; Kato, T. *J. Colloid Interface Sci.* **1976**, *54*, 430.
- (25) Ries, H. E. *J. Colloid Sci.* **1961**, *16*, 361.
- (26) (a) Fujimori, A.; Sugita, Y.; Nakahara, H.; Ito, E.; Hara, M.; Matsuie, N.; Kanai, K.; Ouchi, Y.; Seki, K. *Chem. Phys. Lett.* **2004**, *387*, 345. (b) Fujimori, A.; Araki, T.; Nakahara, H.; Ito, E.; Hara, M.; Ishii, H.; Ouchi, Y.; Seki, K. *Chem. Phys. Lett.* **2001**, *349*, 6.
- (27) Stöhr, J. *NEXAFS Spectroscopy*; Springer: Berlin, 1992.
- (28) Fujimori, A.; Araki, T.; Nakahara, H.; Ito, E.; Hara, M.; Matsuie, N.; Ishii, H.; Ouchi, Y.; Seki, K. *Bull. Chem. Soc. Jpn.* **2003**, *76*, 663.
- (29) Platé, N. A.; Shibaev, V. P. *P. J. Polym. Sci., Macromol. Rev.* **1974**, *8*, 117.
- (30) (a) Fujimori, A.; Saitoh, H.; Shibasaki, J. *J. Polym. Sci., Part A: Polym. Chem.* **1999**, *37*, 3845. (b) Shibasaki, Y.; Nakahara, H.; Fukuda, K. *J. Polym. Sci., Part A: Polym. Chem.* **1979**, *17*, 2387. (c) Shibasaki, Y.; Fukuda, K. *J. Polym. Sci., Part A: Polym. Chem.* **1979**, *17*, 2947. (d) Shibasaki, Y. *J. Polym. Sci., Part A: Polym. Chem.* **1980**, *18*, 1693.
- (31) Fujimori, A.; Masuya, R.; Masuko, T.; Ito, E.; Hara, M.; Kanai, K.; Ouchi, Y.; Seki, K.; Nakahara, H. *Polym. Adv. Technol.* **2006**, *17*, 653.
- (32) (a) Overney, R. M.; Meyer, E.; Frommer, J.; Brodbeck, D.; Luthi, R.; Howald, L.; Guntherodt, H. J.; Fujihira, M.; Takano, H.; Gotoh, Y. *Nature* **1992**, *359*, 133. (b) Imae, T.; Takeshita, T.; Kato, M. *Langmuir* **2000**, *16*, 612. (c) Popovitzbiro, R.; Wang, J. L.; Majewski, J.; Shavit, E.; Leiserowitz, L.; Lahav, M. *J. Am. Chem. Soc.* **1994**, *116*, 1179. (d) Ishida, T.; Yamamoto, S.; Mizutani, W.; Motomatsu, M.; Tokumoto, H.; Hokari, H.; Azehara, H.; Fujihira, M. *Langmuir* **1997**, *13*, 3261.
- (33) Fujimori, A.; Ishitsuka, M.; Nakahara, H.; Ito, E.; Hara, M.; Ishii, H.; Ouchi, Y.; Seki, K. *J. Phys. Chem. B* **2004**, *108*, 13153.